Chemistry of Metals and Alloys

Chem. Met. Alloys 19 (2026) 27-33
ISSN 1998-8079 (print), ISSN 1998-8087 (online)
Ivan Franko National University of Lviv
https://publications.lnu.edu.ua/chemetal

Effect of composition and thermal annealing on the electrochemical performance and durability of mesoporous Pt/Pd-doped TiO_2 composites

Valentina KNYSH[1], Dmytro KOVTUNOV[1], Stanislav SHEMET[1], Serhii CHERNYH[1], Olesia SHMYCHKOVA[1]*, Tatiana LUK'YANENKO[1], Alexander VELICHENKO[1]

[1] *Ukrainian State University of Science and Technologies, Lazaryana St. 2, 49010 Dnipro, Ukraine*
* *Corresponding author. Tel.:* +380567462825; *e-mail: o.b.shmychkova@ust.edu.ua*

Received April 22, 2026; accepted June 25, 2026, available online September 9, 2026
https://doi.org/10.30970/cma19.0462

Mesoporous oxide layers were fabricated on titanium substrates *via* electrochemical anodization. The effects of the composition of the metallic coating (Pt, Pt/Pd) and post-cathodic thermal annealing at 500°C on the electrochemical properties of the resulting composites were systematically studied, including their semiconducting behavior, electrocatalytic performance in oxygen and hydrogen evolution reactions, and long-term durability in 1 M $HClO_4$ aggressive electrolyte. It was found that combined Pt/Pd doping with subsequent heat treatment results in the formation of a stable structure featuring optimal semiconducting parameters (donor density $N = 1.26 \cdot 10^{21}$ cm^{-3}, flat-band potential $E_{fb} = 1.1$ V), which correlates with exceptionally high stability (215 h at 0.5 A). The combined effect of Pt/Pd coating and thermal annealing is shown to ensure better dispersion of catalytic sites and enhanced resistance to degradation as compared to monometallic counterparts.

TiO_2 / Phase composition / Platinum / Palladium / Semiconducting properties / Stability / Heat treatment

1. Introduction

Mesoporous titanium dioxide arrays fabricated by electrochemical anodization have attracted considerable attention as electrode materials for electrocatalysis owing to their high specific surface area, chemical stability, and tunable semiconductor properties [1,2]. Electrochemical anodization is a relatively simple, cost-effective, and scalable fabrication technique that can be performed at relatively low temperatures, making it attractive for the preparation of structured TiO_2 electrodes [3]. Since the pioneering studies of Zwilling and Gong, considerable efforts have been devoted to controlling the anodization parameters to obtain highly ordered nanotubular architectures with high aspect ratios, uniform morphology, and well-defined pore geometry [3,4]. The morphology and physicochemical properties of anodically formed TiO_2 are strongly affected by the applied voltage, electrolyte composition, particularly the fluoride-ion and water content, anodization time, and temperature [3,5]. As-prepared anodic TiO_2 is generally amorphous; therefore, post-anodization thermal treatment is commonly required to induce crystallization. The thermal treatment conditions strongly influence the resulting phase composition, defect structure, and electronic properties of the oxide layer [6,7].

Despite these advantages, the relatively wide band gap of TiO_2 (~3.2 eV for anatase) and its low intrinsic electrical conductivity limit its performance in electrocatalytic applications [8,9]. Surface modification with noble metals, particularly Pt and Pd, represents an effective approach to overcoming these limitations [9,10]. The incorporation of Pt and Pd nanoparticles onto the TiO_2 surface or within its porous structure can provide additional catalytically active sites, facilitate interfacial charge transfer, and modify the semiconductor properties of the oxide [11,12]. In particular, Pd can promote a more uniform dispersion of Pt and suppress its agglomeration, thereby contributing to the preservation of the active surface and the long-term stability of the catalyst [11]. Moreover, bimetallic Pt–Pd systems may exhibit synergistic effects, resulting in enhanced catalytic activity and improved resistance to poisoning by reaction intermediates compared with the corresponding monometallic systems [11,12]. Thermal treatment may further modify the metal-oxide interface and promote redistribution or diffusion of metal species

within the oxide matrix, thereby affecting the concentration of charge carriers and the flat-band potential of the semiconductor [7,13].

Nevertheless, the relationship between the composition of the noble-metal coating, thermal treatment, semiconductor properties, and electrocatalytic behavior of mesoporous TiO_2 has not yet been fully established. In particular, understanding how these parameters affect both the charge-transport characteristics and the long-term stability of TiO_2-based electrodes is essential for their rational optimization.

Therefore, the aim of this study was to systematically investigate the effect of noble-metal coating composition (Pt and Pt/Pd) and thermal treatment on the physicochemical and electrochemical properties of mesoporous TiO_2-based composites. Particular emphasis is placed on correlating the semiconductor parameters, including the donor concentration and flat-band potential, with electrocatalytic activity and long-term electrode stability in an acidic electrolyte under aggressive operating conditions.

2. Experimental

All chemicals were analytical reagent grade. Composites were obtained by the original method, which includes the stages of preliminary preparation of the titanium substrate [13]. Next, the Ti-containing substance grew as TiO_2 after a two-step anodization and cathodization process [14-16] and galvanic platinization. Platinum was electrodeposited from a nitrite platinizing electrolyte [17]. The coating thickness was approximately 1 μm (corresponding to ~2 mg Pt cm^{-2}). Pd was deposited from a phosphate-based palladium-plating electrolyte. The samples were thermally treated in air using a tube furnace at 500°C for 3 h.

The surface morphology was studied by scanning electron microscopy (SEM) with a Tescan Vega 3 LMU with an energy-dispersive X-ray microanalyzer Oxford Instruments Aztec ONE with X-Max^{N}20 detector. X-Ray powder diffraction (XRPD) data were collected in the transmission mode on a STOE STADI P diffractometer with Cu $K\alpha_1$-radiation, a curved Ge (1 1 1) monochromator on the primary beam, $2\theta/\omega$-scan, angular range for data collection 20.000-110.225°2θ with an increment of 0.015, linear position-sensitive detector with a scan step of 0.480°2θ and time per step 75-300 s, U = 40 kV, I = 35 mA, T = 298 K. A calibration procedure was performed using SRM 640b (Si) and SRM 676 (Al_2O_3) NIST standards. Preliminary data processing and X-ray qualitative phase analysis were performed using STOE WinXPOW and PowderCell program packages. The crystal structures of the phases were refined by the Rietveld method with the program FullProf.2k, applying a pseudo-Voigt profile function and isotropic approximation for the atomic displacement parameters, together with quantitative phase analysis.

Electrochemical measurements were performed in a standard three-electrode cell using a VersaSTAT 3A potentiostat-galvanostat (AMETEK Scientific Instruments, USA). The semiconductor properties were determined from Mott-Schottky analysis at a frequency of 1000 Hz in 1 M $HClO_4$. Oxygen and hydrogen evolution reactions were investigated by steady-state polarization. All potentials were measured and are reported against an Ag/AgCl/KCl(sat.) reference electrode.

Four types of electrodes were prepared (electrode area: 1 cm^2): (1) TiO_2-Pt (2 mg cm^{-2}), without thermal treatment; (2) TiO_2-Pt (2 mg cm^{-2}) + thermal treatment in air (500°C, 3 h); (3) TiO_2-Pt (2 mg cm^{-2}) + Pd (1 mg cm^{-2}), without thermal treatment; (4) TiO_2-Pt (2 mg cm^{-2}) + Pd (1 mg cm^{-2}) + thermal treatment in air (500°C, 3 h).

The stability of the electrodes was evaluated under galvanostatic conditions at a current of 0.5 A until significant degradation occurred.

3. Results and discussion

Surface morphology and structure

SEM images of all the samples revealed a well-ordered structure (Fig. 1), which is typical of anodized TiO_2 [17]. Metallic platinum particles are visible on the surface. However, without thermal treatment, the distribution is likely less homogeneous, and some degree of particle agglomeration or clustering is observable compared to the heat-treated samples. Thermal treatment at 500°C did not result in significant deformation or collapse of the coating, in agreement with literature data indicating its thermal stability up to approximately 600-700°C. The heat treatment appears to have facilitated surface diffusion of the Pt particles. While the distribution is improved compared to the untreated Pt-only sample (Fig. 1a), some minor agglomeration may still be present, though the particles are beginning to spread more evenly across the surface and into the upper nanotube layers. The addition of palladium to the platinum coating, even without heat treatment (Fig. 1c), seems to promote a better initial dispersion of the metallic phase compared to the Pt-only sample (Fig. 1a). Agglomeration is reduced, but the metallic species are likely resting primarily on the top surface of the oxide rather than being fully integrated. Sample 4 (Fig. 1d) exhibits the most homogeneous distribution of metallic particles. There is no visible agglomeration of the Pt/Pd bimetallic system. The synergistic effect of Pd addition and thermal treatment results in finely dispersed, uniformly distributed catalytic centers. The particles appear to be located on the surface and are also partially embedded into the upper layers of the TiO_2, creating a well-integrated and highly accessible catalytic surface.

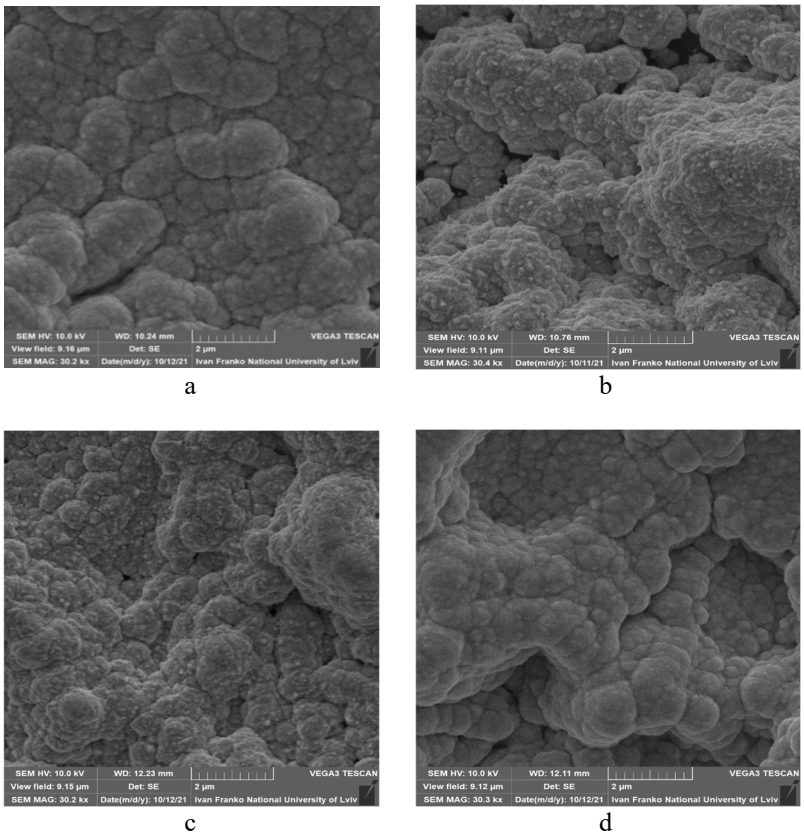


Fig. 1 SEM-images of TiO_2-based composites as prepared: (a) TiO_2-Pt (2 mg cm^{-2}), without thermal treatment; (b) TiO_2-Pt (2 mg cm^{-2}) + thermal treatment in air (500°C, 3 h); (c) TiO_2-Pt (2 mg cm^{-2}) + Pd (1 mg cm^{-2}), without thermal treatment; (d) TiO_2-Pt (2 mg cm^{-2}) + Pd (1 mg cm^{-2}) + thermal treatment in air (500°C, 3 h).

X-ray diffraction data revealed that the resulting nanotubes contain a significant amount of X-ray amorphous compounds on their surface, most likely hydrated titanium oxides. The primary crystalline phase present is titanium dioxide in the anatase form. There are trace amounts of metallic titanium on the surface. Thermal treatment of this material at 500°C for 3 h in an air atmosphere leads to an increase in the proportion of the crystalline phase [13,18]. All the anodes annealed at 500°C show the presence of the anatase phase alone. In the samples loaded with Pd, palladium exists in metallic form and oxide form. Pt exists in metallic form in all samples.

Semiconductor properties

Impedance measurements were carried out in order to investigate the semiconducting properties of the samples involved.

If the surface region of the semiconductor electrode in the investigated potential range is depleted of majority carriers, the experimental data obtained by measuring the electrode capacitance should be linear in coordinates of $C^{-2} - E$ and follow the Mott-Schottky equation [18]:

$$C^{-2} = \frac{2}{e\varepsilon\varepsilon_0 N}(E - E_{fb} - \frac{kT}{e}), \quad (1)$$

where C is the capacitance of the electrode; e is the electron charge; N is the carrier concentration; E_{fb} is the flat-band potential; k is the Boltzmann constant; T is the absolute temperature; ε is dielectric constant and ε_0 is the electric constant.

When $N > 10^{20}$ cm^{-3}, the capacitance of the space-charge layer becomes comparable to the Helmholtz capacitance (approximately 20 μF cm^{-2}). Because these capacitances are connected in series, the $1/C^2$ plot is significantly shifted toward more negative potentials. Therefore, to determine the true flat-band potential, a positive Helmholtz correction must be applied to the extrapolated potential:

$$C^{-2} = C_H^{-2} + \frac{2}{e\varepsilon\varepsilon_0 N}(E - E_{fb} - \frac{kT}{e}), \quad (2)$$

so

$$E_{fb} = E_{C^{-2}=0} + \frac{e\varepsilon\varepsilon_0 N}{2C_H^2} - \frac{kT}{e}. \quad (3)$$

The corresponding semiconductor parameters obtained from Mott-Schottky plots of the investigated anodic TiO_2 films are summarized in Table 1.

The flat-band potentials for all the samples fall within a narrow range of 0.97-1.10 V *vs.* Ag/AgCl reference electrode. All the samples exhibited positive slopes in the Mott-Schottky plots, confirming their n-type semiconductor behavior, which is characteristic

Table 1 Semiconductor properties (N – carrier concentration, E_{fb} – flat-band potential) of TiO_2-based composites as prepared: (1) TiO_2-Pt (2 mg cm^{-2}), without thermal treatment; (2) TiO_2-Pt (2 mg cm^{-2}) + thermal treatment in air (500°C, 3 h); (3) TiO_2-Pt (2 mg cm^{-2}) + Pd (1 mg cm^{-2}), without thermal treatment; (4) TiO_2-Pt (2 mg cm^{-2}) + Pd (1 mg cm^{-2}) + thermal treatment in air (500°C, 3 h).

Sample	N/ cm^{-3}	E_{fb}/ V *vs*. Ag/AgCl	E_{fb}/ V *vs*. RHE
1	2.76×10^{22}	1.06	1.257
2	3.07×10^{22}	1.1	1.297
3	2.94×10^{22}	0.97	1.167
4	1.26×10^{21}	1.1	1.297

of TiO_2 nanotubes and has been widely reported for anodically formed TiO_2 structures [19-21].

The investigation revealed that annealing at 500°C results in only a slight increase in the apparent donor density. At the same time, the flat-band potential shifted from 1.06 to 1.10 V *vs*. Ag/AgCl, corresponding to 1.257 and 1.297 V *vs*. RHE, respectively. The relatively small change in both parameters indicates that thermal treatment of the Pt-modified TiO_2 electrode does not fundamentally alter its semiconductor character. The observed changes may be associated with thermally induced modification of the TiO_2 defect structure, crystallinity, and surface-state distribution [20,22].

A different effect was observed after the introduction of Pd. The TiO_2-Pt-Pd electrode exhibited an apparent donor density of 2.94×10^{22} cm^{-3}, which was close to that of the TiO_2-Pt electrode (2.76×10^{22} cm^{-3}). In contrast, its flat-band potential shifted negatively from 1.06 to 0.97 V *vs*. Ag/AgCl, corresponding to a shift from 1.257 to 1.167 V *vs*. RHE. Thus, Pd incorporation affected the apparent flat-band potential without producing a substantial change in the donor density. This behavior suggests that the effect of Pd is primarily associated with modification of the surface and interfacial electronic structure, rather than with a major change in the concentration of bulk donor defects. Similar changes in the flat-band potential have been reported for metal-modified TiO_2 systems and have been related to metal/semiconductor interfacial charge redistribution and surface-state effects [23-25].

The effect of thermal treatment was much more pronounced for the TiO_2-Pt-Pd electrode. After annealing at 500°C, the apparent donor density decreased from 2.94 10^{22} to 1.26 10^{21} cm^{-3}, corresponding to an approximately 23-fold decrease. At the same time, the flat-band potential shifted positively from 0.97 to 1.10 V *vs*. Ag/AgCl (from 1.167 to 1.297 V *vs*. RHE). Remarkably, the resulting flat-band potential was essentially identical to that of the annealed TiO_2-Pt electrode.

The simultaneous decrease in apparent donor density and positive shift of the flat-band potential indicates a substantial modification of the electrically active surface and near-surface states during the thermal treatment. Annealing can induce structural ordering of anodically formed TiO_2, modify the concentration and distribution of defect states, and alter the metal/TiO_2 interfacial structure [22,26]. In the present Pt-Pd-containing system, thermal treatment may additionally promote redistribution and stronger interaction of the deposited metal species with the TiO_2 surface. Data obtained by X-ray powder diffraction and X-ray photoelectron spectroscopy confirmed that palladium exists predominantly as PdO after annealing at 500 °C in air. This oxidation is critical for understanding the passivation of oxygen vacancies and the resulting decrease in donor density observed by the Mott-Schottky analysis.

The approximately 23-fold decrease in the apparent donor density should therefore not be interpreted as direct evidence for an equivalent decrease in the bulk concentration of oxygen vacancies. For porous and nanostructured TiO_2 electrodes, the capacitance measured by electrochemical impedance spectroscopy may contain contributions from surface and interface states, and the resulting Mott-Schottky parameters should consequently be considered apparent values [20,21]. Changes in the accessibility and electronic activity of these states can strongly affect the slope of the Mott-Schottky plot.

The preservation of a similar E_{fb} value for the annealed TiO_2-Pt and TiO_2-Pt-Pd electrodes, despite their substantially different apparent donor densities, suggests that the thermal treatment drives the two systems toward a similar interfacial electronic state. The lower apparent donor density of the annealed TiO_2-Pt-Pd electrode may correspond to a wider depletion region within the TiO_2, according to the conventional depletion approximation. Such an increase in the space-charge region can potentially favor spatial separation of photogenerated charge carriers.

Electrocatalytic activity and stability

Fig. 2 shows quasi-stationary current-potential curves for electrodes in the potential range where an oxygen evolution reaction (OER) takes place.

The calculated Tafel slopes for the OER were 122, 114, 172, and 94 mV dec^{-1} for electrodes 1-4, respectively. The lowest Tafel slope was obtained for sample 4, indicating more favorable OER kinetics compared with the other electrodes. This enhanced kinetic behavior may be associated with the combined presence of Pt and Pd and with the effect of thermal treatment on the electronic properties of the TiO_2-based

substrate. The Pt/Pd combination may provide a higher diversity of catalytically active sites and facilitate interfacial charge transfer. In addition, thermal treatment can modify the defect structure and electronic properties of the oxide support, potentially contributing to improved OER kinetics. However, direct evidence of a specific Pt-Pd synergistic effect would require further structural and spectroscopic characterization.

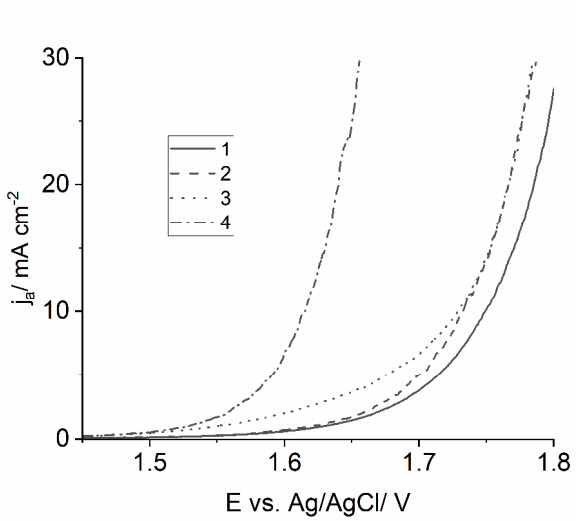


Fig. 2 Quasi steady-state polarisation curves for TiO_2-based composites as prepared: (1) TiO_2-Pt (2 mg cm^{-2}), without thermal treatment; (2) TiO_2-Pt (2 mg cm^{-2}) + thermal treatment in air (500°C, 3 h); (3) TiO_2-Pt (2 mg cm^{-2}) + Pd (1 mg cm^{-2}), without thermal treatment; (4) TiO_2-Pt (2 mg cm^{-2}) + Pd (1 mg cm^{-2}) + thermal treatment in air (500°C, 3 h).

The Tafel slopes for the hydrogen evolution reaction (HER) were 105, 98, 102, and 75 mV dec^{-1} for electrodes 1-4, respectively. As observed for the OER, electrode 4 exhibited the lowest Tafel slope, indicating the most favorable HER kinetics among the investigated electrodes. The improved HER performance can be attributed to a combined effect of the Pt/Pd-containing surface layer and the thermally modified TiO_2 substrate, which may facilitate electron transfer and provide energetically favorable sites for hydrogen evolution. Thus, electrode 4 demonstrates enhanced bifunctional electrocatalytic activity toward both oxygen and hydrogen evolution.

Accelerated durability tests performed at a constant current of 0.5 A revealed pronounced differences in the operational stability of the electrodes. The corresponding operation times were 21 h for electrode 1, 9 h for 2, 8 h for 3, and 215 h for 4.

Electrode 4 exhibited exceptionally high durability, with an operational lifetime approximately 10-27 times longer than those of electrodes 1-3. This result indicates that the combination of Pt/Pd deposition and subsequent thermal treatment substantially enhances the long-term stability of the electrode.

The relatively low stability of electrodes 2 and 3 suggests that neither thermal treatment of the Pt-containing electrode alone nor the deposition of Pt/Pd without subsequent thermal treatment is sufficient to ensure prolonged operation under the applied conditions. For electrode 2, degradation may be related to thermal restructuring, including agglomeration or sintering of Pt species, which can reduce the electrochemically active surface area and potentially weaken the adhesion of the catalytic layer. For electrode 3, the lower stability may be associated with insufficient interfacial stabilization of the deposited metallic components and their possible electrochemical dissolution or redistribution under acidic operating conditions.

The markedly improved durability of electrode 4 may be related to the formation of a more strongly integrated TiO_x-Pt/Pd interfacial structure during the thermal treatment. Such interfacial modification could improve the adhesion of the noble-metal-containing layer to the oxide substrate and mitigate structural changes during prolonged electrochemical operation. The modified interface may also facilitate charge transfer and reduce local mechanical and electrochemical stresses. Nevertheless, the formation of a distinct TiO_x-Pt/Pd interlayer and its proposed protective role should be considered a hypothesis unless directly confirmed by appropriate structural and surface analyses.

The results demonstrate that the electrochemical performance and durability of mesoporous TiO_2-based electrodes are strongly influenced by the metal composition and the metal-oxide interfacial state. The exceptional durability of the annealed Pt/Pd-modified electrode is likely associated with improved integration of the metallic phase, modification of the TiO_2 defect structure, and stabilization of the metal-oxide interface. Further spectroscopic and structural studies are required to establish the detailed mechanism of this stabilization.

Conclusions

All the investigated electrodes exhibited n-type semiconductor behavior. The combination of Pt/Pd modification and annealing at 500°C produced the most pronounced changes in the apparent semiconductor parameters, decreasing the donor density from 2.94×10^{22} to 1.26×10^{21} cm^{-3} while shifting the flat-band potential from 0.97 to 1.10 V *vs*. Ag/AgCl. These changes are consistent with substantial modification of the electrically active surface and near-surface states. Thermal treatment substantially improved the distribution and integration of the metallic phase on the TiO_2 surface. The Pt/Pd-containing electrode after annealing exhibited the most homogeneous distribution of metallic species, with no pronounced agglomeration observed by SEM.

Electrode 4 (TiO_2-Pt/Pd, annealed at 500°C) showed the most favorable electrocatalytic kinetics for both OER and HER, with Tafel slopes of 94 and 75 mV dec^{-1}, respectively. This indicates that the combined Pt/Pd modification and thermal treatment provide favorable conditions for charge transfer and electrocatalytic reactions. The most significant improvement was observed in electrode durability. At a constant current of 0.5 A, electrode 4 operated for 215 h, compared with 21, 9, and 8 h for electrodes 1, 2, and 3, respectively. Thus, the combination of Pt/Pd modification and thermal treatment increased the operational lifetime by approximately one order of magnitude or more, compared to the other investigated electrodes.

The Pt/Pd-modified and thermally treated TiO_2 electrode represents the most promising candidate among the investigated systems, combining enhanced OER/HER kinetics with exceptionally high durability under strongly acidic conditions. These findings highlight the importance of simultaneously controlling noble-metal composition and thermal modification of the oxide support for the development of durable bifunctional electrocatalysts.

References

[1] P. Roy, S. Berger, P. Schmuki, *Angew. Chem. Int. Ed.* 50(13) (2011) 2904-2939. https://doi.org/10.1002/anie.201001374

[2] R. Lee, A. Mazare, P. Schmuki, *Chem. Rev.* 114(19) (2014) 9385-9454. https://doi.org/10.1021/cr500061m

[3] E. Szaniawska-Bialas, A. Brudzisz, A. Nasir, E. Wierzbicka, *Molecules* 29(23) (2024) 5638. https://doi.org/10.3390/molecules29235638

[4] Yi. Zeng, M. Motola, *Chem. Eng. J. Adv.*, 22 (2025) 100752. https://doi.org/10.1016/j.ceja.2025.100752

[5] D. Boykobilov, S. Thakur, A. Samiev, A. Nasimov, K. Turaev, S. Nurmanov, J. Prakash, O. Ruzimuradov, *Inorg. Chem. Commun.* 170(3) (2024) 113419. https://doi.org/10.1016/j.inoche.2024.113419

[6] P. Acevedo-Pena, J.E. Carrera-Crespo, F. Gonzalez, I. Gonzalez, *Electrochim. Acta* 140 (2014) 564-571. https://doi.org/10.1016/j.electacta.2014.06.056

[7] V.O. Knysh, O.B. Shmychkova, T.V. Luk'yanenko, A.B. Velichenko, *Theor. Exp. Chem.* 60 (2025) 420-426. https://doi.org/10.1007/s11237-025-09844-w

[8] K.M. AlAqad, *Ionics* 31(7) (2025) 6601-6633. https://doi.org/10.1007/s11581-025-06408-9

[9] A. Lavacchi, M. Bellini, E. Berretti, Ya. Chen, A. Marchionni, H.A. Miller, F. Vizza, *Curr. Opin. Electrochem.* 28 (2021) 100720. https://doi.org/10.1016/j.coelec.2021.100720

[10] M. Pisarek, P. Kedzierzawski, M. Andrzejczuk, M. Holdynski, A. Mikolajczuk-Zychora, A. Borodzinski, M. Janik-Czachor, *Materials* 13(5) (2020) 1195. https://doi.org/10.3390/ma13051195

[11] Y. Lei, G. Zhao, X. Tong, M. Liu, D. Li, R. Geng, *ChemPhysChem* 11 (2010) 276-284. https://doi.org/10.1002/cphc.200900628

[12] T. Sharifi, T. Mohammadi, M.M. Momeni, H. Kusic, M. Kraljic Rokovic, A. Loncaric Bozic, Y. Ghayeb, *Catalysts* 11(2) (2021) 212. https://doi.org/10.3390/catal11020212

[13] O. Shmychkova, T. Luk'yanenko, A. Velichenko, *Chem. Met. Alloys* 16 (2023) 37-42. https://doi.org/10.30970/cma16.0432

[14] Y. Yang, M.R. Hoffmann, *Environ. Sci. Technol.* 50 (2016) 11888-11894. https://doi.org/10.1021/acs.est.6b03540

[15] M. Chen, C. Wang, Y. Wang, X. Meng, Z. Chen, W. Zhang, G. Tan, *Electrochim. Acta* 323 (2019) 134779. https://doi.org/10.1016/j.electacta.2019.134779

[16] O. Kasian, T. Luk'yanenko, A. Velichenko, R. Amadelli, *Int. J. Electrochem. Sci.* 7 (2012) 7915-7926. https://doi.org/10.1016/S1452-3981(23)17964-8

[17] P.Y. Simons, F. Dachille, *Acta Crystallogr.* 23 (1967) 334-336. https://doi.org/10.1107/S0365110X67002713

[18] V. Knysh, O. Shmychkova, T. Luk'yanenko, A. Velichenko, *Vopr. Khim. Khim. Tekhnol.* 3 (2023) 86-93. https://doi.org/10.32434/0321-4095-2023-148-3-86-93

[19] I. Hanzu, T. Djenizian, P. Knauth, *J. Phys. Chem.*115 (2011) 5989-5996. https://doi.org/10.1021/jp1111982

[20] H. Zhu, M. Zhao, J. Zhou, W. Li, H. Wang, Z. Xu, L. Lu, L. Pei, Z. Shi, S. Yan, Z. Li, Z. Zou, *Appl. Catal. B: Environ*. 234 (2018) 100-108. https://doi.org/10.1016/j.apcatb.2018.04.040

[21] H. Ge, H. Tian, Ya. Zhou, S. Wu, D. Liu, X. Fu, X.-M. Song, X. Shi, X. Wang, N. Li, *ACS Appl. Mater. Interfaces* 6(4) (2014) 2401-2406. https://doi.org/10.1021/am404743a

[22] K. Syrek, A.Sennik-Kubiec, J. Rodriguez-Lopez, M. Rutkowska, P. Zmudzki, K.E. Hnida-Gut, J. Grudzien, L. Chmielarz, G.D. Sulka, *Int. J. Hydrogen Energy* 45(7) (2020) 4376-4389. https://doi.org/10.1016/j.ijhydene.2019.11.213

[23] D. Permporn, R. Khunphonoi, J. Wilamat, P. Khemthong, P. Chirawatkul, T. Butburee, W. Sangkhun, K. Wantala, N. Grisdanurak, J. Santatiwongchai, P. Hirunsit, W. Klysubun, M.D.G. de Luna, *Nanomaterials (Basel)*, 12(3) (2022) 474. https://doi.org/10.3390/nano12030474

[24] A.C. Sola, P. Ramirez de la Piscina, N. Homs, *Catal. Today*, 341 (2020) 13-20. https://doi.org/10.1016/j.cattod.2018.06.017
[25] T. Dittrich, V. Zinchuk, V. Skryshevsky, I. Urban, O. Hilt, *J. Appl. Phys.*, 98 (2005) 104501-104506. https://doi.org/10.1063/1.2135890
[26] J. Lincho, E. Domingues, P. Mazierski, M. Miodynska, T. Klimczuk, A. Zaleska-Medynska, R.C. Martins, J. Gomes, *Sep. Purif. Technol.*, 326 (2023) 124747. https://doi.org/10.1016/j.seppur.2023.124747

Authors and ORCID IDs:
Valentina KNYSH: 0000-0003-3024-3372
Dmytro KOVTUNOV: 0009-0005-5888-4288
Stanislav SHEMET: 0009-0002-8607-9495
Serhii CHERNYH: 0009-0002-3565-4189
Olesia SHMYCHKOVA: 0000-0001-9490-9706
Tatiana LUK'YANENKO: 0000-0001-9272-0301
Alexander VELICHENKO: 0000-0003-1076-9991

The paper is distributed under the terms of the Creative Commons Attribution Non-Commercial 4.0 (CC BY-NC) international license.